



The effect of surface roughness of seed on the high-rate homoepitaxial growth of CVD single-crystal diamonds

Yanyan Zhang¹ · Dongliang Zhang¹ · Libin Zhang² · Bo Yang^{3,4} · Shengnan Shen^{5,6} · Zhiyin Gan^{1,7}

Received: 26 January 2023 / Accepted: 13 April 2023 / Published online: 13 May 2023
© The Author(s), under exclusive licence to Springer-Verlag GmbH, DE part of Springer Nature 2023

Abstract

Although diamond seeds are generally polished before growth, the effect of surface roughness of diamond seeds on crystal growth quality is rarely studied. In this research, three diamond seeds were prepared for researching the effect of surface roughness of diamond seed. They were made by cutting a bulk diamond and subsequently suffered partially polished, totally polished and unpolished, respectively. After a period of microwave plasma chemical vapor deposition growth, various tests were carried out on the samples. According to the microscope and step profiler, the surface roughness of diamond seed did not affect the surface roughness of long-term growth diamonds. Compared by Raman spectra, ultraviolet – visible and infra-red spectra, it indicated that a certain rough surface of diamond seed could improve the internal stress of diamond, but reduce the crystalline quality slightly. Moreover, the surface roughness had almost no impact on the optical properties of the diamond. As a result, diamond seeds with low roughness after cutting could be used for direct growth without polishing, bringing on significant economic for gem-quality diamond production.

Keywords Surface roughness · Diamond seed · MPCVD · Diamond growth

1 Introduction

Diamond has attracted much attention for its excellent physical, optical, thermal and electrical properties, such as a high mechanical hardness of 100 GPa, a wide spectral transparency of about 70% from UV to far IR, a high thermal conductivity of 20 W/(cm·K), a high carrier mobility of 4500 cm²/V·s for electrons and 3800 cm²/V·s for holes and a large energy bandgap of 5.47 eV [1–6]. It can be applied to lathe tools, the jewellery industry, heat–sink devices, photon/particle detection and the semiconductor

industry [7–11]. For the scarcity of natural diamonds, high pressure high temperature growth (HPHT) and microwave plasma chemical vapor deposition (MPCVD) methods have been developed as two promising ways of producing artificial diamonds [12, 13]. Gem-quality diamonds with a big size grown by the MPCVD method have been commercialized successfully [14]. The factors influencing diamond crystal growing quality, including temperature, gas flow rate, pressure, microwave power and auxiliary gas, have been discussed in detail [15–19]. Although diamond seeds are generally polished before

✉ Bo Yang
yb_hust@hust.edu.cn

✉ Shengnan Shen
shen_shengnan@whu.edu.cn

✉ Zhiyin Gan
ganzhiyin@hust.edu.cn

¹ School of Mechanical Science and Engineering, Huazhong University of Science and Technology, Wuhan 430074, People's Republic of China

² School of Mechanical Engineering and Automation, Wuhan Textile University, Wuhan 430074, People's Republic of China

³ CAS Center for Excellence in Quantum Information and Quantum Physics, University of Science and Technology of China, Hefei 230026, People's Republic of China

⁴ CAS Key Laboratory of Microscale Magnetic Resonance and School of Physical Sciences, University of Science and Technology of China, Hefei 230026, China

⁵ School of Power and Mechanical Engineering, Wuhan University, Wuhan 430072, People's Republic of China

⁶ Wuhan University Shenzhen Research Institute, Shenzhen 518057, People's Republic of China

⁷ TrueOne Semiconductor Technology Company Ltd, Guangdong 528251, People's Republic of China

growth, the surface roughness of diamond seeds is rarely mentioned affecting the crystal growth quality.

Recently, researches on growth on the surface of diamond microstructure had been proposed to improve diamond crystal growth quality. Hideo Aida et al. studied the diamond growth mechanism on diamond microneedles and achieved a stress-free layer of the diamond above the diamond microneedles [20, 21]. Tao et al. prepared nanorods on the surface of diamond seeds to grow high-quality CVD diamond layers. They noticed that the diamond seed with optimized nanorods pattern exhibited a smooth surface, lower stress and defect density [22]. Growing on the patterned microstructures surface of diamond seed could improve the diamond quality. However, does a rough surface with random patterns have a similar effect?

In the paper, three diamond seeds were prepared by laser cutting a bulk diamond for the growth experiment. Before growth, they were partially polished, totally polished and unpolished, respectively. According to the microscope and step profiler, diamond surface morphology and surface roughness were recorded. The Raman spectra, ultraviolet – visible (UV – Vis) and infra-red (IR) spectra were collected to judge long-term growth diamonds' crystalline quality and optical properties.

2 Experimental procedures

All experiments were carried out in a homemade commercial 2.45 GHz MPCVD reactor by collaborating with Guangdong TrueOne Semiconductor Technology Co., Ltd. A bulk (100) – oriented single-crystal diamond was grown in MPCVD by a diamond seed (EDP Corporation, Japan), whose size was 7.5 mm × 7.8 mm × 3.4 mm. Three samples with a thickness of 0.5 mm were achieved by cutting the bulk diamond on a LASER SUPRA532 diamond cutting machine (STPL, India). Sample A was partially polished by a polishing machine, and half of the area was polished. Sample B was totally polished. Sample C did not suffer any polishing treatment. The three samples were cleaned with boiling concentrated sulfuric acid, followed by acetone, ethyl alcohol, and deionized water in the ultrasonic bath. Drying the samples on a heating platform was achieved at 80° centigrade for 5 min before growth. Once the MPCVD chamber gate was closed, the vacuum chamber was continuously pumped out through a molecular pump for 2 h to reach a base pressure of $\sim 10^{-6}$ mbar. Before growth, the pressure in the chamber was set 160 mbar and the H₂ gas flow rate was 550 sccm, the samples were etched by H plasma for 2 h to remove the surface damage. After etching, the pressure in the chamber was set 200 mbar, and 37 sccm for CH₄. The whole process of this experimental procedure is shown in Fig. 1.

To explore the initial process of growth, the sample A grew for only 1 h. The sample B and C grew in the

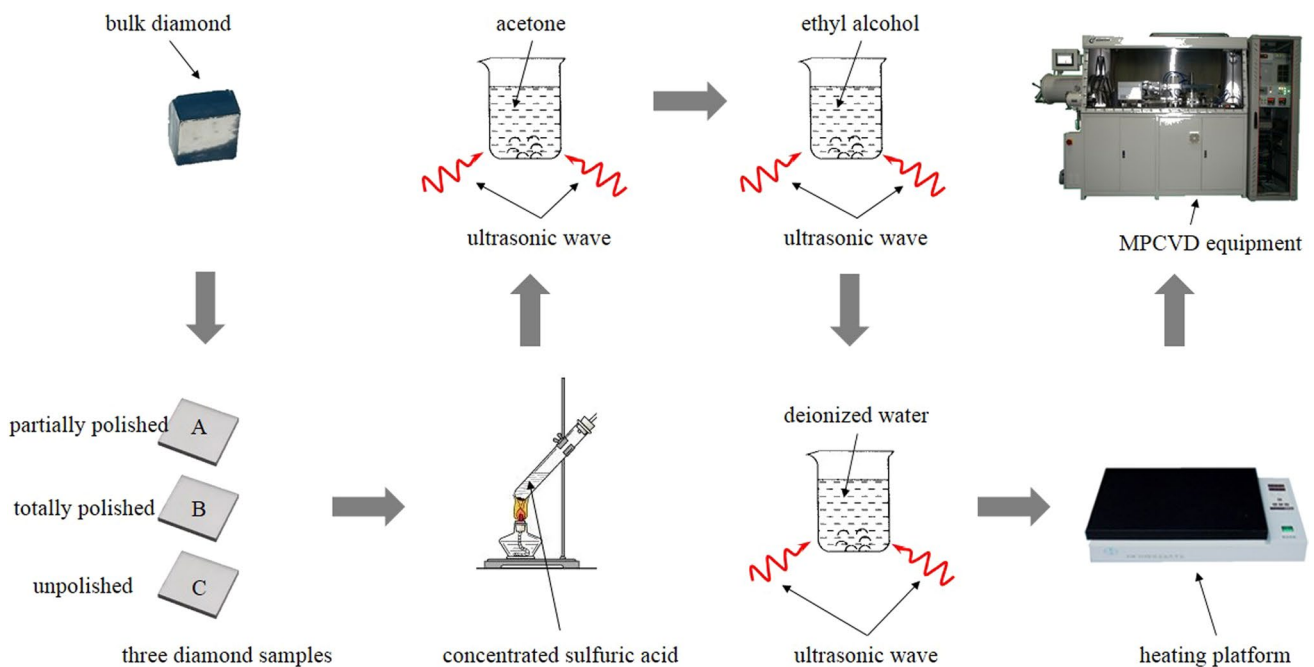


Fig. 1 Whole process of the experimental procedure

same chamber for 150 h with a high rate of about 7 $\mu\text{m}/\text{h}$. The growth conditions of all samples are summarized in Table 1. During the experiment, the crystal quality of the three samples was assessed by recording their Raman spectra using a HORIBA LabRAM HR Evolution spectrometer (HORIBA, France) excited by a solid-state laser at 532 nm with a spot size of 2 μm . The surface profile data were collected using a Dektak XT probe step profiler (Bruker, Germany) with a 30 μN force applied on the microneedle and a scanning distance of 5 mm. The surface morphologies of the samples were examined using a VHX – 600 digital optical microscope (Keyence, Japan) at a magnification of 500x. The UV – Vis transmission spectra of all samples were recorded using a SolidSpec-3700 spectrophotometer (Shimadzu, Japan) over a scan range of 200 – 800 nm. The IR transmission spectra of all samples were recorded using a Nicolet iS50R Fourier transform

infrared spectrometer (Thermo Scientific, America), with a scanning range of 2000 cm^{-1} to 6000 cm^{-1} .

3 Results and discussion

3.1 Surface morphology and surface roughness

The optical image of the surface depicted in Fig. 2a, b illustrates Sample A prior to its growth. Figure 2a displays the cut area, while Fig. 2b displays the polished area. These figures provide a visual representation of the initial state of Sample A. Figure 2a reveals the presence of several strips resulting from laser cutting. In contrast, Fig. 2b appears dark, as the polished surface reflects light with ease. These observations suggest that the polishing process has effectively altered the surface properties of the material. Upon completion of the growth process, a surface image of the interface between the growth area

Table 1 Growth conditions of all samples

Sample ID	Thickness (mm)	H ₂ /CH ₄ gas flow rate (sccm)	Temperature (°C)	Pressure (mbar)	Growth duration (hours)
Sample A	0.502	550/37	950	200	1
Sample B*	0.496	550/37	950	200	150
Sample C*	0.513	550/37	950	200	150

*The sample B and C grew in the same chamber

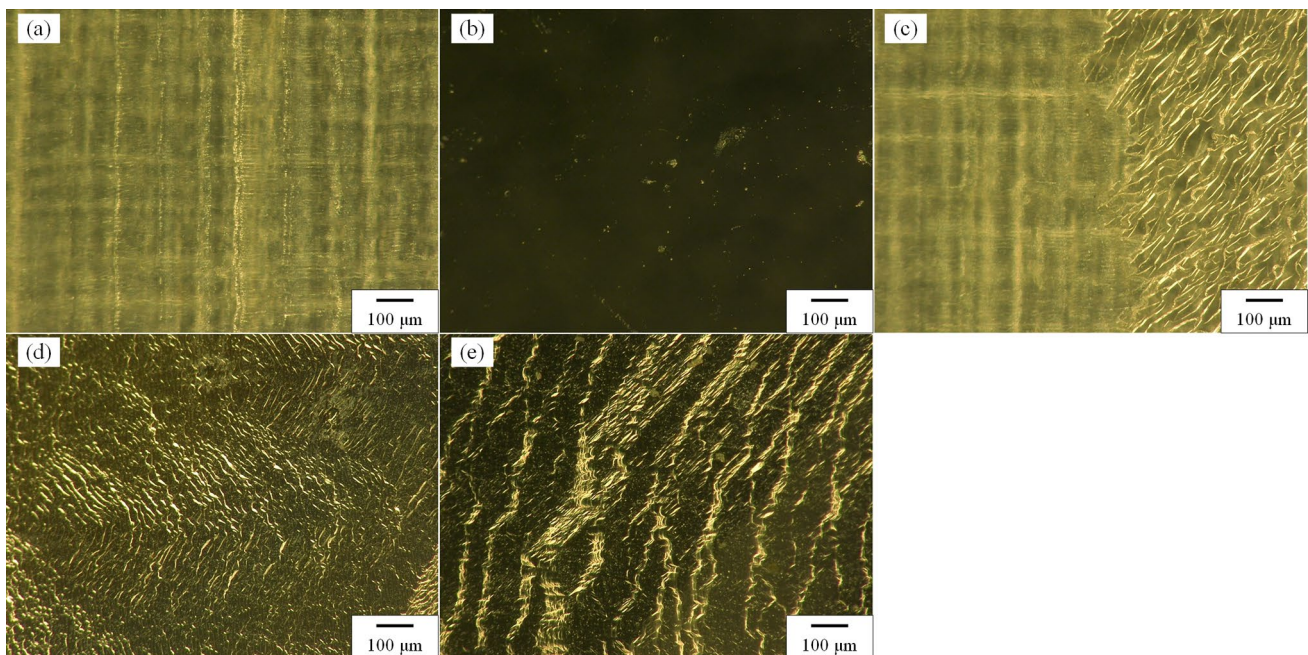


Fig. 2 **a** Surface morphology of the cut area of sample A before growth; **b** surface morphology of the polished area of sample A before growth; **c** surface morphology of an interface between the

growth area and cut area of sample A after growth 1 h; **d** surface morphology of sample B after growth; **e** surface morphology of sample C after growth

and the cut area was obtained after 1 h, as depicted in Fig. 3c. Notably, the figure on the right side of Fig. 3c illustrates the characteristic step-flow growth mode of CVD diamond, which is observed in the experiment [23]. Nevertheless, the left area remained as a cut surface, and it appeared that the partially polished diamond sample had a preference for growth from the polished side. This observation suggests that the polishing process has a significant impact on the growth characteristics of the diamond material. The profiles of Sample A before and after 1 h of growth are presented in Fig. 3a. The figure clearly depicts significant peak-to-valley profiles resulting from laser cutting between 0 and 2 mm. Moreover, the tilt of the polished area observed in the figure is consistent with the actual polishing condition. To facilitate a comparison of the thickness before and after growth, the average thickness calculated from 0 to 3.5 mm is established as the uniform baseline. Notably, the difference in the average thickness calculated between 3.5 and 5 mm is found to be $7.39 \mu\text{m}$. It is apparent that the polished region of the diamond sample exhibits a preference for growth. This phenomenon can be attributed to the epitaxial lateral overgrowth (ELO) mechanism of diamond [24]. The rough surface of a diamond tends to undergo epitaxial lateral overgrowth initially, followed by the stacking of diamond layers, after the uneven diamond surface is connected to form a smooth plane. Hence, after 1 h of growth, the cutting areas on the surface of Sample A do not exhibit the characteristic

step-flow growth mode, while the polished areas of the surface show the characteristic step-flow growth mode.

After 150 h of growth, the surface morphologies of Samples B and C are examined and are presented in Figs. 2d and e, respectively. After a thorough analysis of the figures, it is apparent that they exhibit the characteristic step-flow growth pattern of CVD diamond. The step-flow pattern observed in Fig. 2d appears to be denser and more uniform in comparison with that shown in Fig. 2e. Figure 3b, c exhibits the surface profiles of sample B and C, respectively, both before and after the growth process. Ra and Rz are used to characterize the surface roughness of sample B and sample C, where Ra represents the arithmetic mean deviation of the surface profile, Rq represents the root mean square of the surface profile, while Rz represents the maximum height difference of the surface profile. The mathematical models used to calculate all evaluated parameters are shown from Eqs. (1), (2) and (3) [25]:

$$Ra = \frac{1}{l} \int_0^l |Z(x)| dx \quad (1)$$

$$Rq = \frac{1}{l} \sqrt{\int_0^l Z^2(x) dx} \quad (2)$$

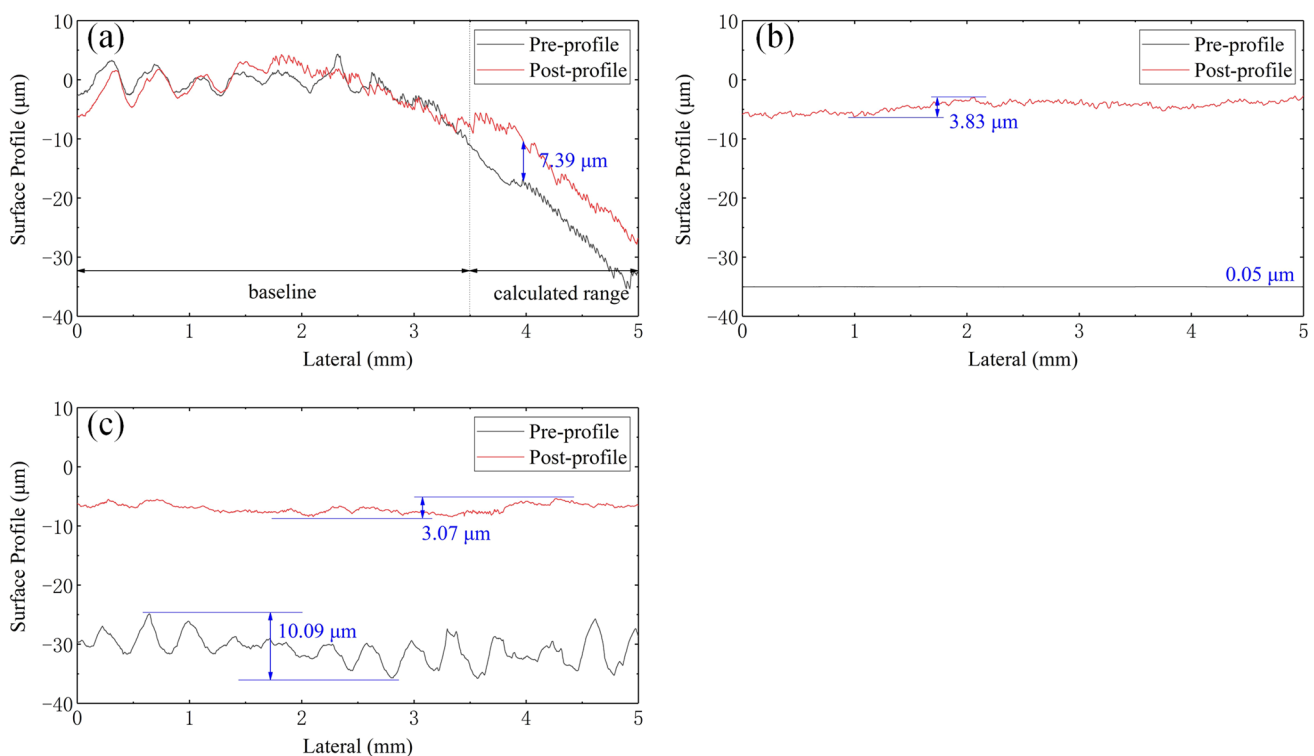


Fig. 3 **a** Surface profile of sample A before and after growth; **b** surface profile of sample B before and after growth; **c** surface profile of sample C before and after growth

$$Rz = Zp_s + Zv_s \quad (3)$$

where $Z(x)$ represents the values of the ordinates of the profile points in the sampling length l . Zp_s represents the maximum height of the profile peaks, while Zv_s represents the greatest depth of the profile valleys. These values are both determined within the sampling length l . Table 2 presents the Ra, Rq, and Rz values acquired for sample A and B, utilizing $l=5$ mm (with profiles collected via probe step profiler) and $dx=0.001$ mm parameters. The Ra, Rq, and Rz values for the polished surface of sample B before growth were $0.007 \mu\text{m}$, $0.004 \mu\text{m}$, and $0.05 \mu\text{m}$, respectively. In contrast, the unpolished surface of sample C exhibited Ra, Rq, and Rz values of $1.76 \mu\text{m}$, $0.99 \mu\text{m}$, and $10.09 \mu\text{m}$, respectively. It can be observed that the surface of diamond that has been polished is smoother compared to the surface which has not been polished. Following a growth period of 150 h, the Ra, Rq and Rz values for sample B were found to be $0.72 \mu\text{m}$, $0.38 \mu\text{m}$ and $3.83 \mu\text{m}$, respectively, and for sample C, the values were $0.63 \mu\text{m}$, $0.33 \mu\text{m}$ and $3.07 \mu\text{m}$, respectively. By comparing the Ra, Rq, and Rz values of the diamond surfaces before and after growth, it can be seen that sample B, which had been polished, became rougher after 150 h of growth, while sample C, which had not been polished, became smoother after 150 h of growth. Despite the Ra, Rq and Rz values for the grown sample C being lower than those of the grown sample B, the difference is insignificant. It appears that after a certain duration of growth, the surfaces of diamond samples, which had differing initial roughness, reached a similar level of roughness. It can be assumed that, when the surface of the diamond sample is relatively flat, the diamond undergoes growth in a layer-by-layer step-flow pattern. When the surface of a diamond is rougher, its initial growth proceeds in accordance with the ELO mechanism until arriving at a sufficiently smooth, flat plane. At this point, the diamond transitions to using the stacking step-flow growth mode. This tendency represents a common pattern in diamond growth, observable particularly when samples differ in initial surface roughness. Therefore, the surface roughness of the diamond seeds do not impact

Table 2 Ra, Rq, and Rz values acquired for sample A and B, utilizing $l=5$ mm (with profiles collected via probe step profiler) and $dx=0.001$ mm parameters

Condition	Parameter	Sample B	Sample C
Before growth	Ra (μm)	0.007	1.76
	Rq (μm)	0.004	0.99
	Rz (μm)	0.05	10.09
After growth	Ra (μm)	0.72	0.63
	Rq (μm)	0.38	0.33
	Rz (μm)	3.83	3.07

the surface roughness of the diamonds produced during long-term growth, which is generally linked to the growth conditions under which the diamonds are produced [26].

3.2 Crystalline quality and optical property

The crystalline quality of all diamond samples was compared by Raman spectra, and the optical property of all samples was judged by UV – Vis and IR transmission spectra. The sampling position of sample A was the polished area and growth area. The Raman spectra of all diamond samples are shown in Fig. 4a. The full width at half maximum (FWHM) and Raman peak are summarized in Table 3. The internal stress of CVD diamond layers can be estimated by the following Raman spectra analysis:

$$P = 0.34 \frac{\text{Gpa}}{\text{cm}^{-1}} \Delta\nu$$

$$\text{with } \Delta\nu = \nu - 1332.5\text{cm}^{-1}$$

where $\Delta\nu$ is the shift of the Raman peak of the diamond layers with respect to the unstressed Raman peak of the diamond [27, 28]. Table 3 shows that the three diamond seeds prior to growth exhibited a very similar tensile stress of 0.01 GPa, as indicated by the Raman peak measured at 1332.47cm^{-1} . Their respective FWHM values were 1.821cm^{-1} , 1.843cm^{-1} , and 1.858cm^{-1} . These preliminary findings provide a useful baseline for assessing any changes in stress and crystalline structure that may result from subsequent growth processes. It is worth noting that the FWHM values of the three samples were all very close to each other, with minimal variation observed. This consistency suggests a high degree of structural uniformity among the samples. For the three samples after growth, the respective Raman spectra peak were at 1332.74cm^{-1} , 1332.02cm^{-1} and 1332.74cm^{-1} , indicating a compression stress of 0.08 GPa, a tensile stress of 0.16 GPa and a compression stress of 0.08 GPa, respectively. The FWHM of the three samples after growth were 1.916cm^{-1} , 1.950cm^{-1} and 2.001cm^{-1} , respectively. In comparison, the internal stress of sample C was lower than that of sample B; however, the FWHM of sample C was wider than that of sample B. In general, CVD diamonds have a certain tensile stress [29], but the unpolished sample C after growth suffered compression stress. It indicated that a certain rough surface of diamond seed could improve the internal stress of the diamond, but reduce the crystalline quality slightly. The view of improving internal stress was also recognized by other researchers [21, 22].

The UV – Vis and IR transmission spectra are shown in Fig. 4b, c. From Fig. 4b, a strong absorption occurred between 200 to 230 nm, and the transmission of all samples between 400 and 800 nm reached approximately 71.2% (theoretical value) [30], indicating that all visible light could

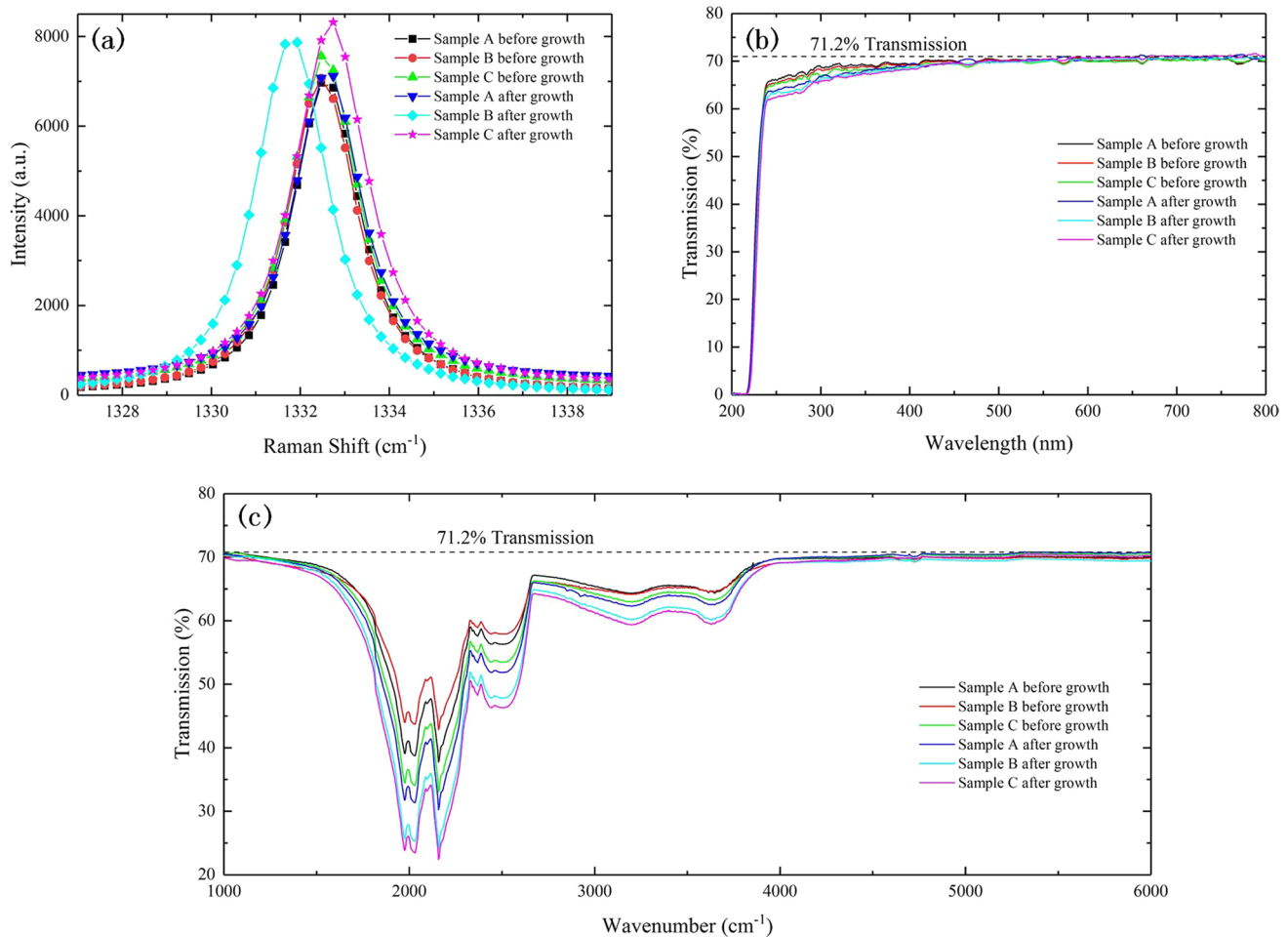


Fig. 4 **a** Raman spectra of all samples before and after growth; **b** UV–Vis transmission spectra of all samples before and after growth; **c** IR transmission spectra of all samples before and after growth

Table 3 FWHM and Raman peak of all samples

Condition	Parameter	Sample A	Sample B	Sample C
Before growth	FWHM (cm^{-1})	1.821	1.843	1.858
	Raman peak (cm^{-1})	1332.47	1332.47	1332.47
After growth	FWHM (cm^{-1})	1.916	1.950	2.001
	Raman peak (cm^{-1})	1332.74	1332.02	1332.74

transmit three samples. From Fig. 4c, the strong bands at 1900 cm^{-1} and 2300 cm^{-1} were the inherent two-phonon lines of a diamond with C–C bonds [31]. In addition, the type absorption lines such as 1282 cm^{-1} , 1370 cm^{-1} and 1330 cm^{-1} were invisible, suggesting that the nitrogen content in all samples was relatively low. Similarly, the transmission of all samples between 4000 cm^{-1} and 6000 cm^{-1} reached approximately 71.2%. Therefore, the optical

properties of all samples before and after growth mainly were the same. The surface roughness had almost no impact on the optical properties of the diamond after growth.

4 Conclusion

In summary, three samples were prepared by cutting a bulk diamond and subsequently suffered partially polished, totally polished and unpolished, respectively. After a period of growth, the growth of the partially polished sample A started from the low areas with a high rate of about 7 $\mu\text{m}/\text{h}$. The surface roughness of long-term growth totally polished sample and unpolished sample were almost the same. As a result, the surface roughness of diamond seed made no effect on the surface roughness of long-term growth diamond. Compared by the Raman spectra, a certain rough surface of diamond seed could improve internal stress of diamond, but reduce the crystalline quality slightly. The UV–Vis

and IR transmission spectra were used to judge the optical properties. The results showed that the surface roughness had almost no impact on optical properties of diamond after growth. Therefore, for gem-quality diamond production, diamond seeds with low roughness after cutting could be used for direct growth without polishing.

Acknowledgements The authors appreciate the kind help of our engineer, Mr. Rongjun Zhang of Guangdong TrueOne Semiconductor Technology Co., Ltd, for support in diamond growth process.

Author contributions YZ: investigation, writing—original draft, validation, data curation; DZ: writing—review and editing, visualization; LZ: software, validation; BY: conceptualization, methodology; SS: funding acquisition, ZG: conceptualization, methodology, funding acquisition.

Funding This work was supported by the National Natural Science Foundation of China (No. 51727901), Guangdong Basic and Applied Basic Research Foundation (No. 2020B1515120005), and Shenzhen Science and Technology Program (JCYJ20220530140603007).

Data availability The data that support the findings of this study are available from the corresponding author upon reasonable request.

Declaration

Conflict of interest The authors declare that they have no known competing financial interests or personal relationships that could have appeared to influence the work reported in this paper.

References

- J. Xiong et al., Mechanical properties evaluation of diamond films via nanoindentation. *Diam. Relat. Mater.* 130, 109403(2022). <https://doi.org/10.1016/j.diamond.2022.109403>
- Y. Cai et al., Continuous-wave diamond laser with a tunable wavelength in orange–red wavelength band. *Opt. Commu.* 528: 128985(2023). <https://doi.org/10.1016/j.optcom.2022.128985>
- Z. Guo et al., Influence of near threshold energy electron irradiation on the thermal conductivity of IIa diamond. *Appl. Phys. Lett.* 119(18), 182105(2021). <https://doi.org/10.1063/5.0067003>
- J. Liu et al., Carrier mobility enhancement on the H-terminated diamond surface. *Diam. Relat. Mater.* 104, 107750(2020). <https://doi.org/10.1016/j.diamond.2020.107750>
- N. Sanders, E. Kioupakis, Phonon-and defect-limited electron and hole mobility of diamond and cubic boron nitride: A critical comparison. *Appl. Phys. Lett.* 119, 062101 (2021). <https://doi.org/10.1063/5.0056543>
- N. Donato, N. Rouger, J. Pernot, G. Longobardi, F. Udrea, Diamond power devices: state of the art, modelling, figures of merit and future perspective. *J. Phys. D: Appl. Phys.* 53(9), 093001(2019). <https://doi.org/10.1088/1361-6463/ab4eab>
- Y. Wei, P. Zhai, X. Chen, L. He, Study on design and diamond turning of optical freeform surface for progressive addition lenses. *Math. Probl. Eng.* 2020, 1–9 (2020). <https://doi.org/10.1155/2020/2850606>
- Q. Lu, H. Gong, Q. Guo, X. Huang, J. Cai, Gemological Characteristic Difference between Colorless CVD Synthetic Diamonds and Natural Diamonds. *Materials* 14(20), 6225(2021). <https://doi.org/10.3390/ma14206225>
- M. Y. Chernykh, et al., GaN-based heterostructures with CVD diamond heat sinks: A new fabrication approach towards efficient electronic devices. *Appl. Mater. Today.* 26, 101338(2022). <https://doi.org/10.1016/j.apmt.2021.101338>
- N.H. Wan et al., Efficient extraction of light from a nitrogen-vacancy center in a diamond parabolic reflector. *Nano Lett.* 18(5), 2787–2793 (2018). <https://doi.org/10.1021/acs.nanolett.7b04684>
- C. De Santi et al., Cause and effects of OFF-state degradation in hydrogen-terminated diamond MESFETs. *IEEE T. Electron Dev.* 67(10), 4021–4026 (2020). <https://doi.org/10.1109/TED.2020.3019018>
- M. Fukuda, M.S. Islam, Y. Sekine, T. Shinmei, L.F. Lindoy, S. Hayami, Crystallization of diamond from graphene oxide nanosheets by a high temperature and high pressure method. *ChemistrySelect* 6(14), 3399–3402 (2021). <https://doi.org/10.1002/slct.202100574>
- R. Ismagilov et al., Single-crystal diamond needle fabrication using hot-filament chemical vapor deposition. *Materials* 14(9), 2320(2021). <https://doi.org/10.3390/ma14092320>
- E. M. Sally, A. Troy, Laboratory-grown diamond: A gemological laboratory perspective. *Journal of Gems & Gemmology*, 23(6), 25–39(2021). <https://doi.org/10.15964/j.cnki.027jgg.2021.06.003>
- C.J. Widmann, W. Müller-Sebert, N. Lang, C.E. Nebel, Homoepitaxial growth of single crystalline CVD-diamond. *Diam. Relat. Mater.* 64, 1–7 (2016). <https://doi.org/10.1016/j.diamond.2015.12.016>
- X. Jia et al., Growth behavior of CVD diamond films with enhanced electron field emission properties over a wide range of experimental parameters. *J. Mater. Sci. Technol.* 34(12), 2398–2406 (2018). <https://doi.org/10.1016/j.jmst.2018.04.021>
- A. Tallaire et al., High NV density in a pink CVD diamond grown with N2O addition. *Carbon* 170, 421–429 (2020). <https://doi.org/10.1016/j.carbon.2020.08.048>
- J. Liu et al., Homo-epitaxial growth of single crystal diamond in the purified environment by active O atoms. *Vacuum* 155, 391–397 (2018). <https://doi.org/10.1016/j.vacuum.2018.06.016>
- P. Balasubramanian et al., Enhancement of the creation yield of NV ensembles in a chemically vapour deposited diamond. *Carbon* 194, 282–289 (2022). <https://doi.org/10.1016/j.carbon.2022.04.005>
- H. Aida, K. Ikejiri, S.W. Kim, K. Koyama, Y. Kawamata, H. Kodama, A. Sawabe, Overgrowth of diamond layers on diamond microneedles: New concept for freestanding diamond substrate by heteroepitaxy. *Diam. Relat. Mater.* 66, 77–82 (2016). <https://doi.org/10.1016/j.diamond.2016.03.019>
- H. Aida et al., Microneedle growth method as an innovative approach for growing freestanding single crystal diamond substrate: detailed study on the growth scheme of continuous diamond layers on diamond microneedles. *Diam. Relat. Mater.* 75, 34–38 (2017). <https://doi.org/10.1016/j.diamond.2016.12.016>
- T. Zhi et al., High quality CVD single crystal diamonds grown on nanorods patterned diamond seed. *Diam. Relat. Mater.* 119, 108605(2021). <https://doi.org/10.1016/j.diamond.2021.108605>
- A. L. Vikharev, M. A. Lobaev, A. M. Gorbachev, D. B. Radishev, V. A. Isaev, S. A. Bogdanov, Investigation of homoepitaxial growth by microwave plasma CVD providing high growth rate and high quality of diamond simultaneously. *Mater. Today Commun.* 22, 100816. (2020). <https://doi.org/10.1016/j.mtcomm.2019.100816>
- Y.H. Tang, B. Bi, B. Golding, Diamond Heteroepitaxial Lateral Overgrowth. *MRS Online Proc. Libr.* 1734, 20–25 (2014). <https://doi.org/10.1557/opl.2015.175>
- J. Dobes et al., Effect of mechanical vibration on Ra, Rq, Rz, and Rt roughness parameters. *Int. J. Adv. Manuf. Technol.* 92, 393–406 (2017). <https://doi.org/10.1007/s00170-017-0137-0>

26. C. Nørgård, S.S. Eskildsen, A. Matthews, The influence of oriented growth on the surface roughness of CVD diamond films. *Surf. Coat. Tech.* **74**, 358–361 (1995). [https://doi.org/10.1016/0257-8972\(95\)08241-7](https://doi.org/10.1016/0257-8972(95)08241-7)
27. G. Wu, M.H. Chen, J. Liao, The influence of recess depth and crystallographic orientation of seed sides on homoepitaxial growth of CVD single crystal diamonds. *Diam. Relat. Mater.* **65**, 144–151 (2016). <https://doi.org/10.1016/j.diamond.2016.03.011>
28. E.J. Di Liscia, F. Álvarez, E.M. Burgos, E.B. Halac, H.A. Huck, M.E. Reinoso, Stress analysis on single-crystal diamonds by Raman spectroscopy 3D mapping. *Mater. Sci. Appl.* **4**(3), 191–197 (2013). <https://doi.org/10.4236/msa.2013.43023>
29. D. Schwarzbach, R. Haubner, B. Lux, Internal stresses in CVD diamond layers. *Diam. Relat. Mater.* **3**(4–6), 757–764 (1994). [https://doi.org/10.1016/0925-9635\(94\)90264-X](https://doi.org/10.1016/0925-9635(94)90264-X)
30. S.E. Coe, R.S. Sussmann, Optical, thermal and mechanical properties of CVD diamond. *Diam. Relat. Mater.* **9**(9–10), 1726–1729 (2000). [https://doi.org/10.1016/S0925-9635\(00\)00298-3](https://doi.org/10.1016/S0925-9635(00)00298-3)
31. H. Liu et al., Single Crystal Diamond Deposited by Dual Radio-Frequency Plasma Jet CVD with High Growth Rate. *Crystals* **9**(1), 32(2019). <https://doi.org/10.3390/cryst9010032>

Publisher's Note Springer Nature remains neutral with regard to jurisdictional claims in published maps and institutional affiliations.

Springer Nature or its licensor (e.g. a society or other partner) holds exclusive rights to this article under a publishing agreement with the author(s) or other rightsholder(s); author self-archiving of the accepted manuscript version of this article is solely governed by the terms of such publishing agreement and applicable law.